ELSEVIER

Coordination Chemistry Reviews
190–192 (1999) 245–265

COORDINATION CHEMISTRY REVIEWS

www.elsevier.com/locate/ccr

Structure–function relationships of copper-containing nitrite reductases

Shinnichiro Suzuki [a,*], Kunishige Kataoka [a], Kazuya Yamaguchi [a], Tsuyoshi Inoue [b], Yasushi Kai [b]

[a] *Department of Chemistry, Graduate School of Science, Osaka University, Toyonaka, Osaka 560-0043, Japan*

[b] *Department of Materials Chemistry, Graduate School of Engineering, Osaka University, Suita, Osaka 565-0871, Japan*

Accepted 17 February 1999

Contents

Abstract . . . 245
1. Introduction . . . 247
2. Spectroscopic characterization of Cu-containing nitrite reductases . . . 249
   2.1 Group 1 . . . 250
   2.2 Group 2 . . . 250
   2.3 Group 3 . . . 250
3. Structures of Cu-containing nitrite reductases . . . 254
4. Functions of Cu-containing nitrite reductases . . . 258
   4.1 Intermolecular electron transfer process . . . 258
   4.2 Intramolecular electron transfer process . . . 259
   4.3 Reduction of nitrite ion . . . 262
5. Conclusion . . . 263
Acknowledgements . . . 263
References . . . 263

Abstract

Dissimilatory nitrite reductase (NIR) is a key enzyme in the anaerobic respiratory pathway of denitrifying bacteria. There are two types of NIR, one of which contains copper and the

* Corresponding author. Tel.: +81-6-6850-5767; fax: +81-6-6850-5785.
E-mail address: bic@ch.wani.osaka-u.ac.jp (S. Suzuki)

PII: S0010-8545(99)00069-7

other heme. Cu-containing NIR (Cu NIR) has the trimeric structure with one type 1 Cu (blue copper) atom and one type 2 Cu (nonblue copper) atom in each subunit. The type 1 Cu atom bound by 2His, Cys, and Met accepts one electron from an electron donor protein and shows an intense color, blue or green. The type 2 Cu atom bound by 3His and a solvent (H_2O or OH^-) is a reduction center of nitrite to NO. The intramolecular long-range electron transfer process is observed from the type 1 site to the type 2 Cu site with a half-life period of ca. 0.3 ms. The present review deals with (i) spectroscopic characterization of Cu NIR's, (ii) structures of Cu NIR's, and (iii) functions of Cu NIR's (intermolecular electron transfer process, intramolecular electron transfer process, and reduction of nitrite ion).

Keywords: Denitrification; Nitrite reductase; Type 1 Cu; Type 2 Cu; Copper proteins; X-ray crystal structure; Long-range electron transfer

Nomenclature

NIR
nitrite reductase

T2D-NIR	type 2 Cu-depleted nitrite reductase
AxgNIR	NIR from *Alcaligenes xylosoxidans* GIFU 1051
AxnNIR	NIR from *Alcaligenes xylosoxidans* NCIB 11015
AciNIR	NIR from *Achromobacter cycloclastes* IAM 1013
AfsNIR	NIR from *Alcaligenes faecalis* S-6
HypNIR	NIR from *Hyphomicrobium* sp.
PsaNIR	NIR from *Pseudomonas aureofaciens*
PssNIR	NIR from *Pseudomonas* sp.G-179
RhhNIR	NIR from *Rhizobium 'hedysari'* strain HCNT1
RhsNIR	NIR from *Rhodobacter sphaeroides* 2.4.3
pAz	pseudoazurin
Aci-pAz	pseudoazurin from *Achromobacter cycloclastes* IAM 1013
Afs-pAz	pseudoazurin from *Alcaligenes faecalis* S-6
Az	azurin
Axg-Az	azurin from *Alcaligenes xylosoxidans* GIFU 1051
Aoase	ascorbate oxidase
His	histidine
Met	methionine
Cys	cysteine
Lys	lysine
Glu	glutamic acid
Asp	aspartic acid
Val	valine

Thr	threonine
CD	circular dichroism
MCD	magnetic circular dichroism
EPR	electron paramagnetic resonance
ENDOR	electron nuclear double resonance
NHE	normal hydrogen electrode

1. Introduction

All organisms need organic nitrogen as a constituent part of the cell. The fixed nitrogen utilizable for organisms is generally poor in the ecosystem, being the suppressed growth factor for many organisms. A recent rapid rise in world population is partly due to the invention of synthetic nitrogen fixation (Haber–Bosch process). In order to keep the environment of the earth constant, fixed nitrogen must be completely reconverted into dinitrogen gas. The reverse process of dinitrogen fixation is denitrification. Fig. 1 shows the terrestrial nitrogen cycle that consists of several linked biological and abiological processes. Denitrification is the dissimilatory reduction of nitrate or nitrite ion usually to produce dinitrogen by prokaryotic organisms [1]. Denitrifying bacteria occupy a wide range of natural habitats including soil and water, and return large amounts of fixed nitrogen to the atmosphere in the natural world. Therefore, we have to rely on denitrifying bacteria to remove inorganic nitrogen compounds as pollutants which bring about air pollution, acidic rain, and water pollution (eutrophication).

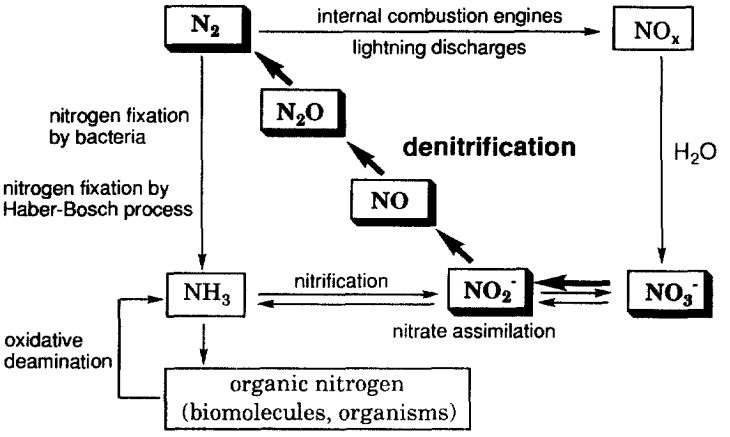

Fig. 1. Terrestrial nitrogen cycle.

In Fig. 1, the denitrification process is a cascade of anaerobic respiration processes which are catalyzed by the corresponding metalloenzymes [1,2]. The first step (two-electron reduction) is carried out by the dissimilatory membrane-bound nitrate reductase containing molybdenum with both heme and non-heme irons. This enzyme is more closely related to the respiratory DMSO reductase of *E. coli* and has an Mo(VI)O center with two dithiolene-containing pterin cofactor ligands [3]. The second step (one-electron reduction) is catalyzed by the dissimilatory soluble enzyme, nitrite reductase (NIR) of which two distinct types are known: hemes c,d_1-containing NIR and Cu-containing NIR. The former is isolated from a large number of bacteria, approximately two-thirds of the denitrifying bacteria examined to date. The dimeric enzyme consists of two domains, a small one including the covalently bound heme c and a large one including the heme d_1 [4,5]. Copper NIR is a trimer, in which the monomer contains one type 1 Cu (blue copper) bound in a subunit and one type 2 Cu (nonblue copper) located between two subunits [6–10a]. The nitric oxide reductase containing hemes b and c is concerned with the third step (two-electron reduction). The reason why the presence of nitric oxide reductase was not ascertained for a long time is that this enzyme is an unstable membrane-bound protein. The protein consists of large and small subunits containing heme c and heme b, respectively [2,11]. The final step (two-electron reduction) is carried out by the soluble copper enzyme, nitrous oxide reductase. The protein is usually a homodimer of 7–9 kDa subunits with 4 Cu/monomer. The oxidized enzyme shows bright purple or pink and changes into typical blue expected for copper proteins after the reduction with dithionite. The spectroscopic studies suggest that the enzyme contains at least one mixed-valent, thiolate-bridged Cu(I)–Cu(II) unit [12], which is similar to the binuclear copper center in cytochrome c oxidase [13,14]. Nitric oxide reductase and nitrous oxide reductase attract special attention because these enzymes might be an ancestor protein of terminal oxidases like cytochrome c oxidase and ubiquinol oxidase [15,16].

About ten Cu NIR's have been characterized so far from a variety of denitrifying bacteria. In 1955, the first Cu NIR was found in the strain of *Alcaligenes xylosoxidans* NCIB 11015, which was isolated from soil at Nagoya University by Iwasaki et al. and was tentatively identified as *Pseudomonas denitrificans* [17,18]. Other such copper enzymes were isolated from *Achromobacter cycloclastes* [19], *Alcaligenes faecalis* S-6 [20], *Bacillus halodenitrificans* [21], *Haloferax denitrificans* [22], *Nitrosomonas europaea* [23], *Pseudomonas aureofaciens* [24], *Rhodobacter sphaeroides* [25], and *Hyphomicrobium* sp. [26]. In the early reports, Cu NIR was not uniform with respect to the number and type of copper species and the subunit structure. The Cu NIR's from *A. xylosoxidans* NCIB 11015 (AxnNIR) [27] and *P. aureofaciens* [24] were reported to be dimeric enzymes (70–85 kDa) and have two type 1 Cu atoms only. The dimeric Cu NIR (69 kDa) from *A. cycloclastes* IAM 1013 (AciNIR) was believed to have both the type 1 and 2 Cu atoms [28]. Moreover, the Cu NIR from *A. faecalis* S-6 (AfsNIR) was described as being a tetramer of 110 kDa, containing four copper atoms distributed in the enzyme as the type 1 and 2 Cu sites [29]. However, X-ray crystal structure analyses of three Cu NIR's revealed that all of AciNIR [6,7], AxnNIR [9,10a], and AfsNIR [8] are

similar trimers with each of the type 1 and 2 Cu atoms per monomer. The paper on the first crystal structure analysis of AciNIR by Adman et al. described a trimer both in the crystal and in solution [6]. It was subsequently concluded that Cu NIR's require both type 1 and 2 Cu's for optimal activities [30,31]. The fourth crystal structure of the Cu NIR from *A. xylosoxidans* GIFU 1051 [32] (AxgNIR) has been recently determined at 2.05 Å resolution [33]. The molecular structure of AxgNIR is also a trimer with two Cu atoms. Two azurins (Az-I and Az-II) with AxgNIR were found in this bacterium as well as *A. xylosoxidans* NCIB 11015 [34]. According to sequence analyses of these Az's composed of 129 amino acid residues, only one residue in each Az from *A. xylosoxidans* GIFU 1051 (Gln106 in Az-I and Val31 in Az-II [35]) is replaced in the corresponding protein from *A. xylosoxidans* NCIB 11015 (Glu106 in Az-I and Met31 in Az-II [36]).

Herein we focus on the structure–function relationships of Cu NIR's which catalyze the dissimilatory reduction of nitrite ion to nitric oxide. In the functions of Cu NIR, three basic reactions are included: intermolecular and intramolecular electron transfer processes and redox reaction. Several physicochemical methods (spectroscopy, electrochemical method, pulse radiolysis, and X-ray crystal analysis) and techniques of protein engineering are very effective for the structure–function studies of Cu NIR's.

2. Spectroscopic characterization of Cu-containing nitrite reductases

The metal binding sites of copper proteins are generally categorized as type 1, type 2, and type 3 Cu's according to their spectroscopic and magnetic properties [37]. Type 1 Cu or blue copper derived from the intense blue color of proteins shows unique spectroscopic properties. This Cu(II) ion exhibits an intense absorption band near 600 nm ($\varepsilon = 2{,}000$–$5{,}000\ M^{-1}\ cm^{-1}$), which is attributable to an allowed ligand-to-metal charge transfer transition [S(Cys)→(Cu(II)]. The EPR spectra of type 1 Cu give small hyperfine coupling constants (3–7 mT). The type 1 Cu center is characterized by a distorted tetrahedral or a trigonal bipyramidal geometry and usually serves as an electron transfer site in mobile electron carrier proteins such as azurin and plastocyanin. In redox Cu-containing enzymes, type 1 Cu accepts electron(s) from an electron donor and then donates them to a reaction center in the same molecule. On the other hand, type 2 Cu or nonblue copper shows weak visible bands in electronic absorption spectra and larger hyperfine coupling constants (12–20 mT) in EPR spectra. These spectral characters are typical of distorted tetragonal coordination. Type 2 Cu is usually involved in the catalytic redox system of the substrate. Type 3 Cu center contains a pair of antiferromagnetically-coupled Cu(II) ions (EPR-silent). Since type 2 and 3 Cu's generally have no Cys ligand, these centers do not show intense colors. Moreover, a new Cu site has been recently found in cytochrome *c* oxidases: a paramagnetic Cu_A site is composed of mixed valence binuclear Cu atoms with two Cys-bridging ligands [13,14].

Copper NIR's are classified into three groups by the spectroscopic properties of type 1 Cu as follows.

2.1. Group 1

Since the type 1 Cu sites of AxnNIR [27,31], AxgNIR [38], and PsaNIR [24] exhibit an intense ca. 590 nm absorption band, NIR's in this group are blue in color. They show EPR signals with an axial symmetry such as those of plastocyanin and azurin [37,39]. It has been recently reported that the Cu NIR from fungus *Fusarium oxysporum* also gives very similar electronic absorption and EPR spectra [40].

2.2. Group 2

AciNIR [19,28], AfsNIR [20], the NIR from *R. sphaeroides* forma sp. *denitrificans* [25,41], and RhsNIR [42] are green or bluish–green enzymes, displaying two intense absorption bands (near 460 and 600 nm) and rhombic EPR signals from the type 1 Cu sites.

2.3. Group 3

Miscellaneous NIR's except the enzymes in groups 1 and 2 belong to group 3. *N. europaea* NIR shows a visible absorption spectrum similar to those of multicopper oxidases [43]. The NIR's from *B. halodenitrificans* [44] and *Hyphomicrobium* sp. [26] also have spectroscopically unique type 1 Cu.

The typical electronic absorption and CD spectra of NIR's (AciNIR, AxgNIR, and HypNIR) in the three groups are shown in Fig. 2, [26,38]. The absorption and CD spectra of type 2 Cu-depleted NIR (T2D-AxgNIR and T2D-AciNIR) prepared by the treatment of the native enzyme with chemical reagents are quite similar to those of the native enzyme, indicating that the type 2 Cu center makes extremely small spectral contribution in the visible region [38]. The absorption bands of the blue NIR, AxgNIR (group 1) appear at 470, 593, and 785 nm in the pH range 6.0–8.5, being the same as those of AxnNIR [45]. The visible spectrum is analogous to that of plastocyanin [39,46]. The unique absorption spectrum of green AciNIR (group 2) displays three intense bands at 460, 589, and 690 nm and a shoulder band around 400 nm. Greenish blue HypNIR (group 3) shows two strong absorption bands at 456 and 605 nm. Moreover, the similar CD extrema of these three NIR's are observed in the visible region, but in AxgNIR and AxnNIR the extrema around 600 nm have a negative sign [38,45]. In plastocyanin having a distorted tetrahedral Cu(II) center, a weak absorption band in the range of 400–500 nm is separated to two peaks (427 and 468 nm) assigned as the Met → Cu(II) and His → Cu(II) charge transfer transitions, respectively [46]. The geometry of the type 1 Cu center in AxgNIR is also distorted tetrahedral (vide infra) [33]. Two transitions appeared at 410 and 477 nm by the curve analysis of AxnNIR [45] would be assigned to the Met → Cu(II) and His → Cu(II) charge transfer transitions, respectively. The most intense absorption band near 600 nm is assigned as the Cys → Cu(II) charge transfer transition and all the d → d transitions are predicted to be lower in energy than 700 nm [46]. The assignment of the absorption bands for HypNIR would be similar to

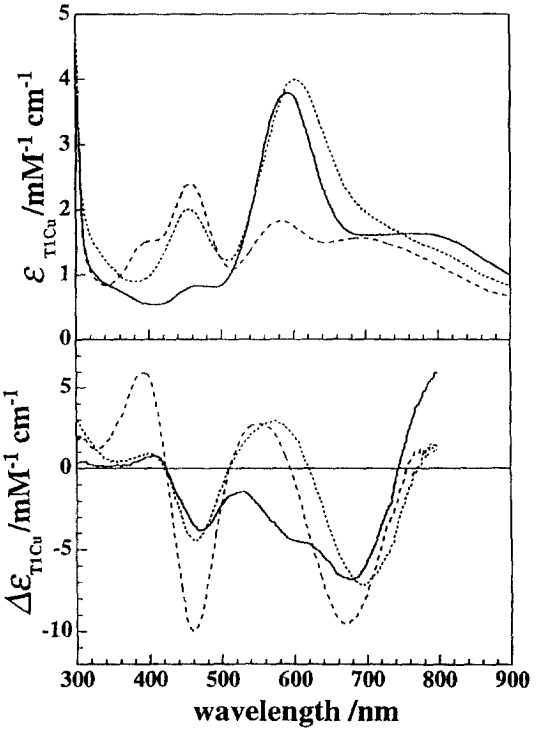

Fig. 2. Electron absorption (upper) and CD (lower) spectra of AxgNIR (solid line), AciNIR (broken line), and HypNIR (dotted line) at pH 7.0.

those for AxgNIR and AxnNIR. On the other hand, two intense bands (460 and 589 nm) of AciNIR having the flattened tetrahedral type 1 Cu center [6,7] are assigned as the Cys→Cu(II) transfer transition and a shoulder near 400 nm is assigned to the Met→Cu(II) transfer transition [46]. The geometric distortion responsible for the electronic structure changes in AciNIR, relative to plastocyanin having a distorted tetrahedral Cu site, is determined to involve a coupled angular movement of the Cys and Met residues toward a more flattened tetrahedral (toward square planar) structure. This movement is consistent with a greater tetragonal Jahn–Teller distortion resulting from the shorter Cu–S(Met) bond in AciNIR compared with the Cu site in plastocyanin: this increased distortion implies that the type 1 Cu site in AciNIR is in a 'less entatic' (or reduced rack) state than in plastocyanin [46].

The EPR spectra of native AxgNIR, AciNIR, and HypNIR at 77 K are depicted with those of the T2D forms of AxgNIR and AciNIR in Fig. 3, [26,38]. Both signals of type 1 and 2 Cu's are observed in the native NIR's. The EPR parameters of rhombic type 1 Cu in AciNIR are $g_z = 2.19$, $A_z = 7.3$ mT, $g_y = 2.06$, $g_x = 2.02$, and $A_x = 4.2$ mT and those of type 2 Cu are $g_z = 2.33$ and $A_z = 13.0$ mT. The axial-type spectra of AxgNIR show the parameters of $g_{/\!/} = 2.22$, $g_\perp = 2.05$, and

$A_{//} = 6.9$ mT (type 1 Cu) and $g_{//} = 2.32$ and $A_{//} = 12.8$ mT (type 2 Cu). The EPR signal of HypNIR also shows an axial symmetry (type 1 Cu, $g_{//} = 2.25$ and $A_{//} = 5.5$ mT; type 2 Cu, $g_{//} = 2.35$ and $A_{//} = 13.0$ mT). Two hyperfine lines of type 2 Cu in the region of 0.26–0.29 T are shifted in the presence of anion (nitrite, azide, or nitrate ion), implying the binding of these ions to the type 2 Cu site [38].

The mutation Met182Thr in which the Met ligand of type 1 Cu was changed to Thr in the NIR from *R. sphaeroides* 2.4.3 (RhsNIR), results in a blue rather than green type 1 Cu center. However, the EPR signal of the mutant is unchanged from that of the native type 1 Cu site [42]. On the other hand, the mutant (Met150Glu) with a replacement of the type 1 Cu ligand, Met150 by Glu in green AfsNIR shows no intense visible absorption band and a type 2-Cu EPR signal only [47].

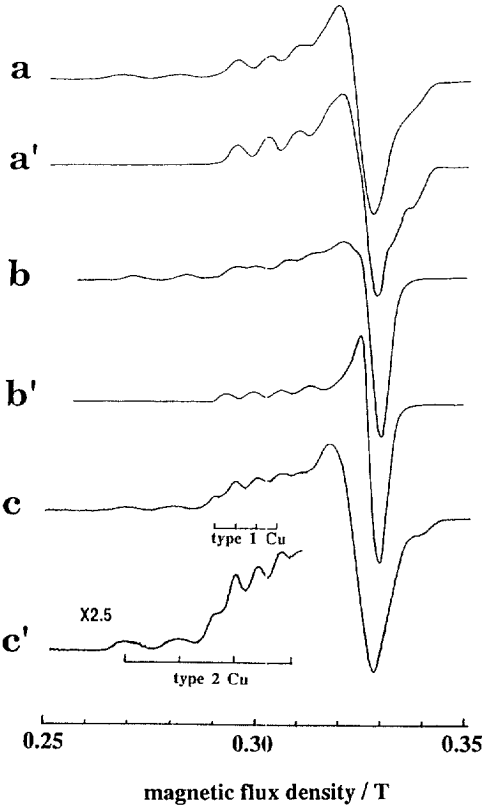

Fig. 3. A 77-K EPR spectra of AciNIR (a), T2D-AciNIR (a'), AxgNIR (b), T2D-AxgNIR (b'), and HypNIR (c and c') at pH 7.0.

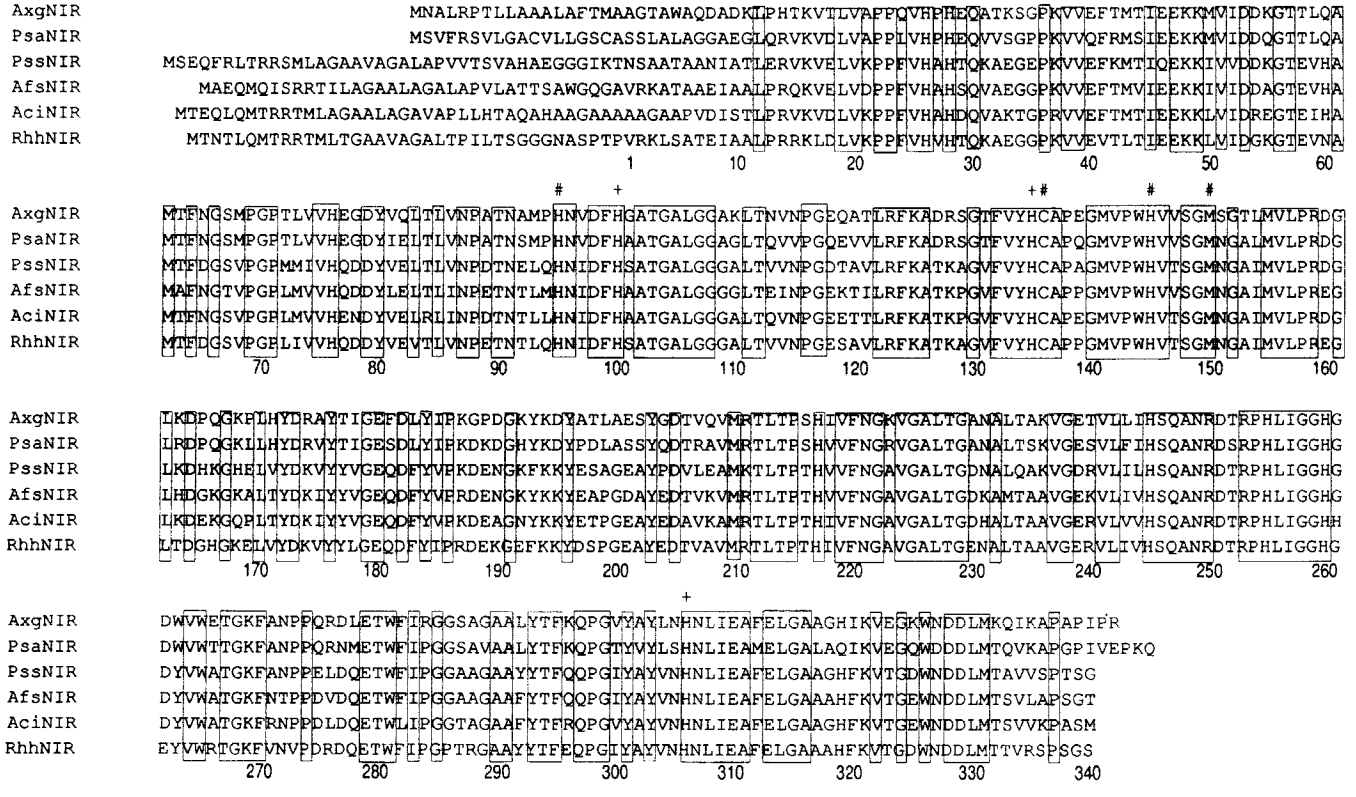

Fig. 4. Sequence alignment of six NIR's. Axg, *A. xylosoxidans* GIFU1051 [48]; Psa, *P. aureofaciens* [49]; Pss, *Pseudomonas* sp. G-179 [50]; Afs, *A. faecalis* S-6 [51]; Aci, *A. cycloclastes* IAM1013 [52]; Rhh, *Rhizobium 'hedysari'* strain HCNT1 [53]; #, type 1 Cu ligand; +, type 2 Cu ligand. Conserved residues are boxed.

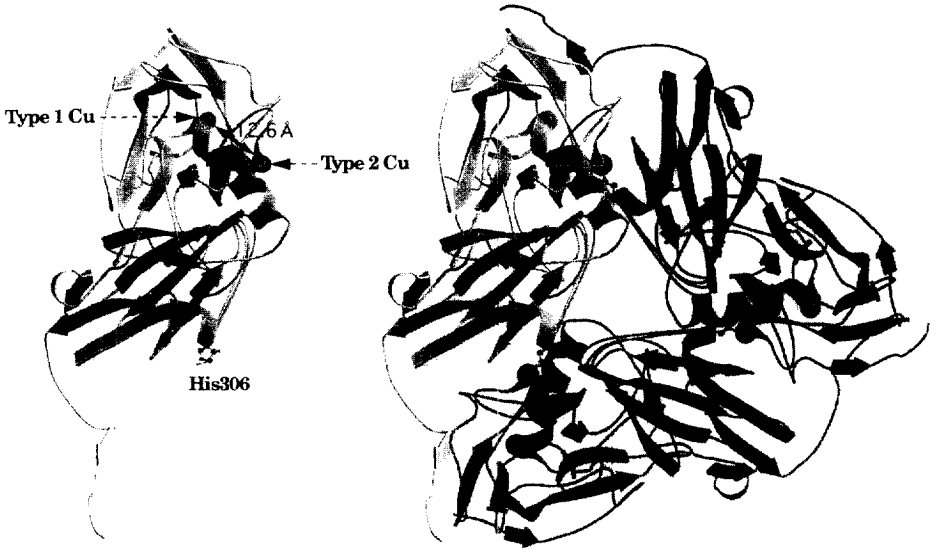

Fig. 5. Molecular structures of monomer (left) and trimer (right) of AxgNIR.

3. Structures of Cu-containing nitrite reductases

The primary structures of two blue NIR's (group 1: AxgNIR and PsaNIR), three green NIR's (group 2: PssNIR, AfsNIR, and AciNIR), and RhhNIR are exhibited in Fig. 4. According to the ca. 80% sequence identity of RhhNIR with the NIR's in group 2, RhhNIR probably has a green color. In the figure, the numbering of the amino acid residues of all NIR's are the same as those of AciNIR [7]. AxgNIR (monomer, 36 kDa) has ca. 80% sequence identity with the other blue NIR's and ca. 70% identity with three green NIR's. Bluish-green RhsNIR has an extra residue between the 140 and 141 amino acid residues of the sequence alignments in Fig. 4, [54]. In the latest paper by Vandenberghe et al. [55] the sequence alignment of AxnNIR was described to be identical with that of AxgNIR except for only one amino acid residue, that is, Val39 in AxgNIR is replaced with Thr39 in AxnNIR [54]. However, Dodd et al. [10a] and Suzuki et al. [10b] reported that the sequence alignment of AxnNIR is completely in agreement with that of AxgNIR.

The first X-ray crystal analysis of Cu NIR was achieved with green AciNIR by Adman et al. [7]. The crystal structures of two green NIR's (AciNIR [7,8] and AfsNIR [8]) and two blue NIR's (AxnNIR [9,10a] and AxgNIR [33]) have so far been analyzed. The four NIR's have quite similar whole structures. The enzyme subunits are tightly associated around a 3-fold axis to form a trimer around a central channel, as shown in Fig. 5. Each subunit has each of type 1 and 2 Cu's. Their polypeptide fold is a 'Greek key' β barrel like as in copper proteins. In one subunit, the β barrels are stacked on each other and there are two short α-helical regions. One of the helixes runs from residue 141 to 149 and contains two type 1 Cu ligands, His145 and Met150.

The His 145 residue bound to the type 1 Cu ion with the N(δ1) atom is oriented such that the N(ε2) atom is exposed to the solvent at the bottom of a small cavity in the protein surface. The Cu atom lies ca. 4 Å from the His145 N(ε2) atom. Surrounding the cavity containing the His145 residue is a flat area of protein surface, with the Cu atom being ca. 7 Å beneath. An electron will be transferred through the cavity from a donor protein to the type 1 Cu(II) site. In the type 1 Cu site, four amino acid residues (His95, Cys136, His145, and Met150) form a flattened tetrahedron (green AciNIR and AfsNIR) or a distorted tetrahedron (blue AxgNIR)

Table 1
Details of the Cu geometries of oxidized NIRs[a]

	Blue NIR		Green NIR	
	Axg	Axn	Aci	Afs
Crystallization	pH 8.5	pH 6.0	pH 5.4	pH 4–4.8
Resolution	2.05 Å	2.1 Å	2.1 Å	2.0 Å
R-factor	0.180	0.181	0.164	0.191
(Type 1 Cu site)				
Cu–His95	2.11	2.07	2.02	2.06
Cu–His145	2.00	1.94	2.02	1.98
Cu–Cys136	2.18	2.20	2.16	2.08
Cu–Met150	2.62	2.62	2.59	2.64
Displacement from 2His and Cys plane	0.6 Å	0.5 Å	ca. 0.4 Å	ca. 0.5 Å
Geometry of type 1 Cu	Distorted tetrahedral	Distorted trigonal planar	Flattened tetrahedral	Flattened tetrahedral
H145–Cu–H95	99	103	99	102
H145–Cu–C136	116	117	103	108
H145–Cu–M150	114	115	129	130
H95–Cu–C136	131	127	134	133
H95–Cu–M150	86	86	88	85
C136–Cu–M150	108	106	108	101
(Type 2 Cu site)				
Cu–H100	2.07	2.07	2.00	1.91
Cu–H135	2.18	2.17	2.04	2.07
Cu–H306	2.27	2.17	2.19	2.09
Cu–WO(water)	2.55	2.26	1.90	2.00
H100–Cu–H135	110		104	99
H100–Cu–H306	94		108	99
H135–Cu–H306	104		111	111
WO–Cu–H100	164		101	148
WO–Cu–H135	81		110	97
WO–Cu–H306	94		121	99

[a] Axg, *A. xylosoxidans* GIFU1051 [33]; Axn, *A. xylosoxidans* NCIB11015 [10a]; Aci, *A. cycloclastes* IAM 1013 [7]; Afs, *A. faecalis* S-6 [8].

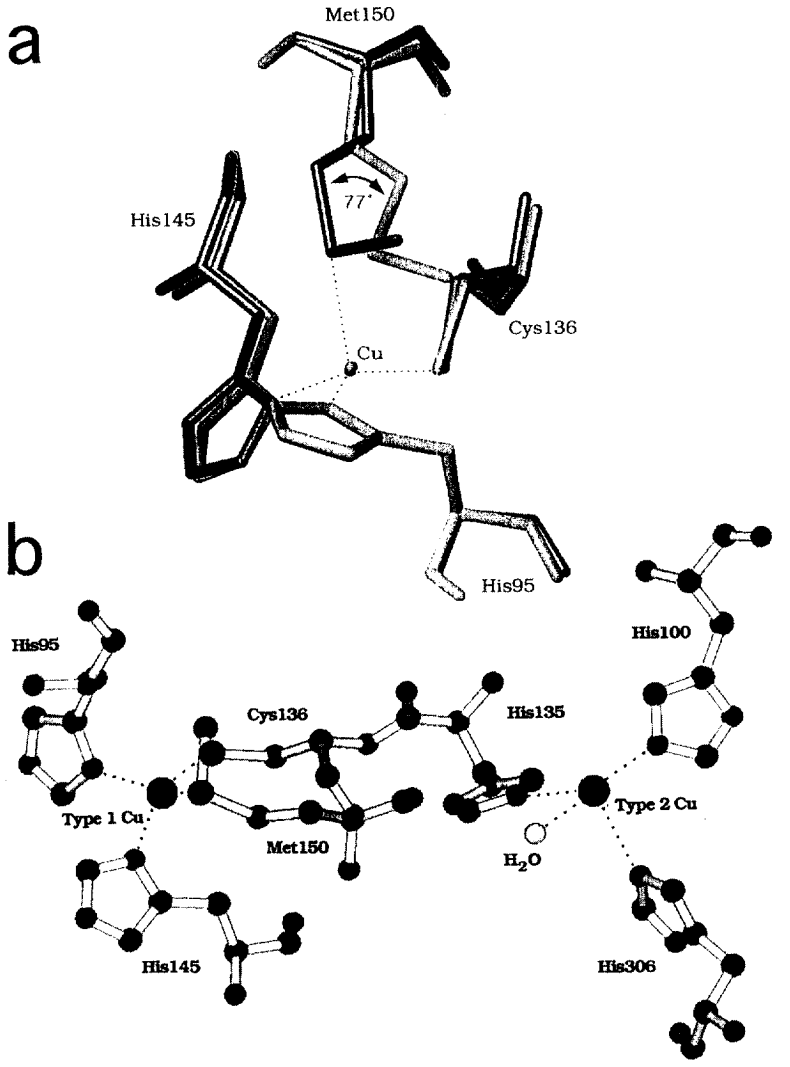

Fig. 6. (a) Superposition of the type 1 Cu sites of AxgNIR (black) and AfsNIR (gray), and (b) structure of type 1 and 2 Cu sites of AxgNIR.

(Table 1). The structure of the type 1 Cu site in AxgNIR is quite similar to that in poplar plastocyanin [56], but it has been reported on blue AxnNIR that the type 1 Cu center is in a distorted trigonal planar geometry [10a]. The superposition of the type 1 Cu sites of AxgNIR and AfsNIR is shown in Fig. 6(a), the superposition was carried out on the three strongly ligating residues (His95N(δ1), His145N(δ1), and Cys136S(γ)). In AxgNIR the displacement of the Cu ion out of the NNS plane defined by 2N(His) and S(Cys) ligands toward S(Met150) is similar to that in AfsNIR (ca. 0.5 Å). The S(Met) ligand of AxgNIR deviates slightly from the axial

position of the NNS plane, while that of AfsNIR is in the considerably tilted position. Both the Cu(II)–S(Met) distances in these NIR's are shorter than that of plastocyanin by ca. 0.2 Å [56]. Moreover, the side chains of the Met ligands are quite different from each other in conformation and the dihedral angle between the planes involving the C(β)–C(γ)–S(δ) side chain is 77° (Fig. 6(a)).

The type 2 Cu atom lies at the bottom of a 12–13 Å deep solvent channel and is the site to which the nitrite ion binds. The type 2 Cu is ligated by three His ligands (His100 N(ε2), His135 N(ε2), and His306 N(ε2)), but His306 comes from the adjacent subunit. Thus, the Cu atom is bound at the interface of two subunits (Fig. 5). In the early reports, the total number of Cu atoms in Cu NIR's were not constant, since the type 2 Cu ion would be partially or considerably removed under drastic conditions such as the enzyme preparation [30,31,38]. The three His ligands of the type 2 Cu site together with a solvent ligand (H_2O or OH^-) form a distorted tetrahedral geometry (Fig. 6(b)), which gives the smaller $A_{//}$ value (12.8 mT) of the type 2 Cu ion in AxgNIR than those of type 2 Cu's in the other Cu proteins [38]. All the His residues remain oriented in the same place even on removal of the type 2 Cu (T2D-NIR) [7]. The type 2 Cu site is suggested to be similar to the Zn(II) site binding three His residues in carbonic anhydrase [57]. The MCD spectra of the Co(II)-substituted type 2 sites in AciNIR and AxgNIR are analogous to those of Co(II)-substituted molluscan hemocyanins involving a tetrahedral Co(II) ion [58].

There is a hydrogen bond network extending from the solvent ligand of the type 2 Cu atom, which involves Asp98 and His255 residues in the vicinity of the Cu atom and is related with nitrite reduction to NO [7–10a]. The solvent ligand is hydrogen bonded to the carboxylate group of Asp98, which in turn forms a H_2O-bridged hydrogen bond to the histidyl nitrogen atom (His255). X-ray crystal structure analysis of nitrite-soaked NIR demonstrated that nitrite ligates the type 2 Cu(II) ion in a bidentate fashion through two oxygens [7–10a]. One of the nitrite oxygens forms a hydrogen bond to one of the carboxylate oxygen atoms of Asp98 (the O–O distance between nitrite oxygen and carboxylate oxygen of Asp, 3.0–3.4 Å) and the other nitrite oxygen is hydrogen bonded to two H_2O molecules [8]. The other carboxylate oxygen atom of Asp98 also forms a H_2O-bridged hydrogen bond to His255 in the vicinity of the type 2 Cu site without the nitrite ligand. In ascorbate-reduced colorless AfsNIR, the H_2O or OH^- ligand at the type 2 Cu(I) ion is no longer present, although the structure of the type 1 Cu site is scarcely changed [8]. The conformation of the three His ligands does not change from the oxidized structure, resulting in a tri-coordinate tetrahedral Cu site. Moreover, the conformations of Asp98 and His255 are not perturbed by the absence of the H_2O or OH^- ligand. In the case of the nitrite-soaked reduced copper, nitrite appears to be coordinated to the type 2 Cu(I) site in the same mode as the oxidized form [8].

The distance between the type 1 and 2 Cu sites in the monomer is 12.6 Å and the bridging ligand between two Cu's is the His135-Cys136 amino acid sequence segment, as shown in Fig. 6(b). This bridging mode between type 1 and 2 Cu's is similar to that between the type 1 Cu site and the trinuclear Cu center composed of one type 2 Cu atom and a couple of type 3 Cu in multicopper oxidases such as laccase [59], ascorbate oxidase [60], and ceruloplasmin [61]. In zucchini ascorbate

oxidase (AOase), the His506-Cys507-His508 amino acid sequence segment links the type 1 Cu ion and the type 3 Cu ions as a bridging ligand: the Cys(507) residue is coordinated to the type 1 Cu ion and the two adjacent His residues bind to each of the type 3 Cu pair [60]. The shortest distance between the type 1 Cu site and the trinuclear Cu center is 12.2 Å and electrons from ascorbate ion transfer from the type 1 Cu center to the trinuclear center through the Cys-His sequence segment.

4. Functions of Cu-containing nitrite reductases

4.1. Intermolecular electron transfer process

NIR requires an electron donor for the one-electron reduction of nitrite. The electron donors of AciNIR [28,62] and AfsNIR [63] in group 2 are a kind of blue copper protein, pAz which shows an intense ca. 590 nm band with two weak bands around 450 and 780 nm, and a rhombic EPR signal [64]. Az is believed to be an electron donor for blue NIR's found in *P. aureofaciens* [24] and *A. xylosoxidans* [36]. The reduced Az from the former strain, transfers an electron efficiently to its cognate NIR [24]. Two Az's from the latter strain also function as donors to AxnNIR, and the progress curves are biphasic, with an initial linear phase followed by an extended nonlinear phase [36]. However, a cytochrome *c* might be an electron donor for *A. xylosoxidans* NIR [27].

Voltammetric study of the electron transfer reaction from Aci-pAz ($pI = 8.6$, $E_{1/2} = +0.26$ V vs. NHE at pH 7.0 [64]) to AciNIR ($pI = 4.6$, $E_{1/2}$(type 1 Cu) = + 0.24 V vs. NHE at pH 7.0 [38]) is shown in Fig. 7, [65]. The pAz accepts an electron from a bis(4-pyridyl)disulfide modified gold electrode and donates it to AciNIR (1/100 equivalents of pAz) in the presence of nitrite ion (Fig. 7, the electron transfer process). The cyclic voltammetric response of Aci-pAz indicates the quasi-reversible electron transfer process (Fig. 7(a)). In the presence of excess nitrite, the shape of the voltammogram changes remarkably and an enhanced sigmoidal cathodic current-potential curve (catalytic current) is observed (Fig. 7(b)). The appearance of the catalytic current implies the regeneration of the oxidized pAz in the diffusion layer. The second-order rate constant of the intermolecular electron transfer from Aci-pAz to AciNIR was estimated to be 7.3 (10^5 M^{-1} s^{-1} at pH 7.0. On the other hand, apo-AciNIR does not change the voltammetric response of Aci-pAz (Fig. 7(c)). In the electron transfer system between Axg-Az(I or II) and AxgNIR, however, the voltammetric responses of two Az's were slightly changed in the presence of the enzyme, indicating the very slow electron transfer processes (unpublished data).

The interaction of pAz with its cognate NIR involves a strong electrostatic element. Afs-pAz (basic protein) has a surface ring of Lys residues (Lys10, Lys38, Lys57, and Lys77) around the blue Cu center, which is required for the electron transfer to AfsNIR [63,66]. There is little change in the k_{cat} values of intermolecular electron transfer reaction on replacement of these Lys residues, but the K_m values increase by a factor of 2–3 [63]. At the AfsNIR surface, the Glu118, Glu197,

Glu204, and Asp205 residues are substantially conserved in green NIR's (Fig. 4). The substitution of their acidic amino acid residues decreases the k_{cat} values and increases the K_m values [66]. It is proposed by X-ray crystal analysis and kinetic analysis of the wild and mutant proteins that the following pairings between the basic amino acid residues of Afs-pAz and the acidic amino acid residues of AfsNIR are possible: Lys10 with Glu197, Lys77 and/or Lys57 with Glu118, and Lys38 with Glu204 and/or Asp205. The type 1 Cu atoms in each would be 14–15 Å apart in the suggested pAz–NIR complex.

4.2. Intramolecular electron transfer process

As shown in Fig. 5, type 1 and 2 Cu's are 12.6 Å apart. One electron donated by an electron carrier at the type 1 Cu site is transferred to the type 2 Cu site through the Cys136-His135 sequence segment (Fig. 6(b)). The intramolecular electron transfer process was successfully observed by a pulse radiolysis experiment [38,67]. Fig. 8 shows the time-course of the absorbance at 590 nm after pulse radiolysis of AxgNIR and that in the presence of nitrite at pH 6.0 [68]. In these room

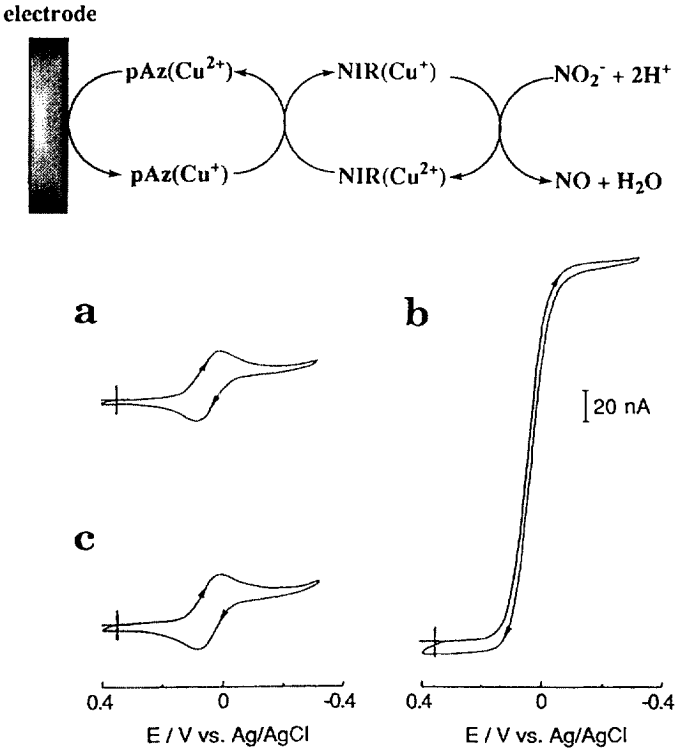

Fig. 7. Electron transfer process for cyclic voltammetry (upper) and cyclic voltammograms of Aci-pAz system in 0.1 M phosphate buffer (pH 7.0) at 25°C (lower). (a) Aci-pAz (100 μM); (b) Aci-pAz after addition of AciNIR (1 μM); (c) pAz after addition of apo-AciNIR (1 μM).

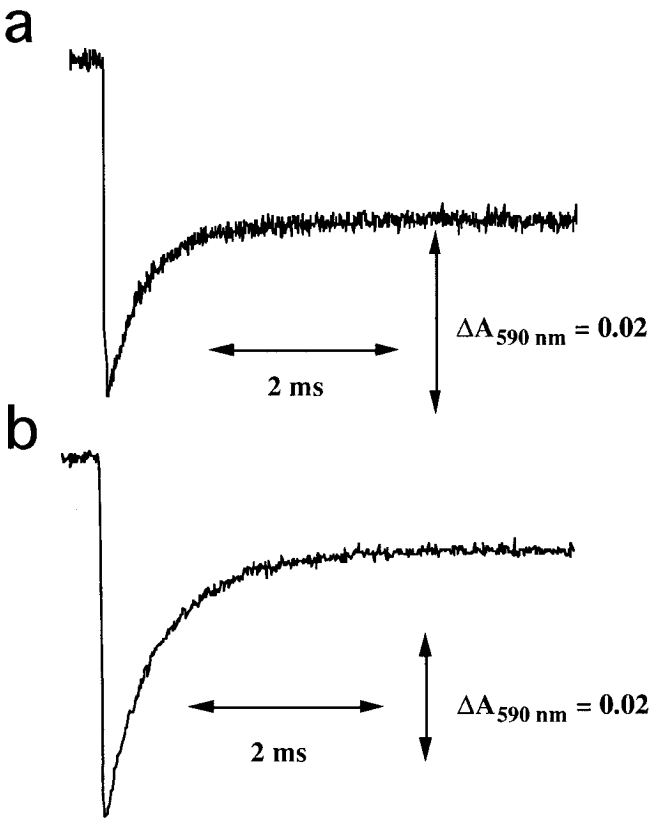

Fig. 8. (a) Time-resolved absorption change of an AxgNIR solution at 25°C ($k_{ET} = 2{,}100\ s^{-1}$) and (b) a in the presence of nitrite ($k_{ET} = 2{,}000\ s^{-1}$). Reaction conditions are as follows: NIR, 102 μM; nitrite, 500 μM; *t*-butyl alcohol, 0.1 M; *N*-methylnicotinamide, 1 mM; 10 mM potassium phosphate buffer (pH 6.1).

temperature spectra, the blue bands quickly disappear after pulse irradiation, indicating that the type 1 Cu sites are reduced with a half-time period of ca. 10 μs. After the reduction, slow recoveries of the absorbance are observed in the sample solutions containing the native enzyme, while the absorbance of T2D-AxgNIR at 590 nm does not recover even after 8 ms. The increased absorbance is held constant at 53% of the total absorbance change in Fig. 8(a). A linear relationship between the amount of type 2 Cu in AciNIR and the absorbance at 460 nm is observed [67]. These results suggest that the recovery process is the intramolecular electron transfer process from the type 1 Cu site to the type 2 Cu site:

$$\mathrm{T1Cu(II)\text{–}T2Cu(II)} \xrightarrow{e^-} \mathrm{T1Cu(I)\text{–}T1Cu(I)\text{–}T2Cu(II)} \underset{k_b}{\overset{k_f}{\rightleftarrows}} \mathrm{T1Cu(II)\text{–}T2Cu(I)}$$

The observed rate constants of the electron transfer reaction (k_{ET}) consists of the sum of k_f (forward) and k_b (backward). In Fig. 8(a and b), the k_{ET} values were estimated to be 2100 and 2000 s^{-1} at pH 6.1, respectively. The k_{ET} values of

AxgNIR and AciNIR in the absence and presence of nitrite are listed in Table 2. The observed k_{ET} values (2100 s^{-1}) of two NIR's at pH 6 indicate a half-life period of 0.3 ms, being about 13 times as large as that of the intramolecular electron transfer process from type 1 Cu to the trinuclear Cu site in zucchini AOase [69,70]. It seems curious that the k_{ET} values in the presence of nitrite are smaller than those in the absence of it at pH 7.0. However, the pH-k_{ET} profiles of AciNIR and AxgNIR indicate the maximum values around pH 6 [68], and those in the presence of nitrite are approximately consistent with the pH-nitrite reduction activity profiles which show the optimal values of pH 5.5–6.0 [19a,71]. Therefore, the intramolecular electron transfer process would be closely linked to the following catalytic reduction process of nitrite.

The redox potentials of the type 1 and 2 Cu centers in AxgNIR and AciNIR were estimated by cyclic voltammetry [72] and pulse radiolysis [38], (Table 2). The type 1 Cu potential of AciNIR is close to the +0.26 V midpoint potential of Aci-pAz at pH 7.0. The midpoint potential (+0.20 V at pH 7.0) of T2D-AciNIR is slightly shifted to negative potential [72] compared with that of native AciNIR. The differences between two potentials of type 1 and 2 Cu's are small (20–40 mV). However, RhsNIR in group 2 has the +0.247 V type 1 Cu midpoint potential and the type 2 Cu reduction potential is below +0.200 V in the absence of nitrite [42]. Therefore, reduction of the type 2 Cu(II) site by the type 1 Cu(I) site is not energetically favored, but it is suggested that the binding of nitrite to the type 2 Cu(II) center is the trigger positively shifting the type 2 Cu reduction potential and induces catalytic electron transfer reaction. Moreover, the mutation Met182Thr in which the Met ligand of type 1 Cu is changed to Thr, resulted in a blue rather than blue–green type 1 Cu, the midpoint potential of +0.345 V, and a somewhat reduced NIR activity [42].

Table 2
Observed intramolecular electron transfer rate constants (k_{ET}) and redox potentials ($E°$) of AxgNIR and AciNIR at 25°C[a]

NIR's	pH	k_{ET}/s^{-1}	$E°$/V (vs. NHE)	
			Type 1 Cu	Type 2 Cu
AxgNIR	6.1	2100	+0.29	+0.31
AxgNIR + nitrite	6.1	2000		
AxgNIR	7.0	1900	+0.28	+0.25
AxgNIR + nitrite	7.0	320		
AciNIR	6.0	2100	+0.27	+0.29
AciNIR + nitrite	6.0	1900		
AciNIR	7.0	1400	+0.24	+0.28
AciNIR + nitrite	7.0	650		

[a] NIR, 100–200 μM; nitrite, 500 μM.

4.3. Reduction of nitrite ion

The cyclic voltammetry of AciNIR exhibits well defined voltammetric response at a modified gold electrode in the presence of its cognate apo-pAz as a mediator [72]. From the relative catalytic currents at various nitrite concentrations, the second-order rate constant of nitrite reduction (k) and the Michaelis constant (K_m) of AciNIR were shown to be 5×10^2 $M^{-1}s^{-1}$ and 7×10^{-4} M at pH 7.0 and 25°C, respectively. The k and K_m values of T2D-AciNIR are 1×10^2 $M^{-1}s^{-1}$ and 3×10^{-3} M, respectively. The measurement of the enzyme activity of AciNIR by colorimetric method also indicated that the reduction activity of T2D-NIR is equal to half the activity of the native enzyme at pH 6.0 [38]. On the other hand, the relationship between the activity and the Cu content of AciNIR was extrapolated to zero activity for the enzyme containing only 3 Cu per trimer (T2D NIR) [30]. The catalytic activity of T2D-NIR is still controversial.

The EPR-measurement of native Cu NIR in the presence of an anion (nitrite, azide, and nitrate) implies that these ions bind to the type 2 Cu(II) site [38]. X-ray crystal structure analyses of nitrite-soaked crystals of AciNIR [7], AfsNIR [8], and AxnNIR [9,10a] also demonstrated that nitrite replaces a solvent bound to the type 2 Cu site and binds via its oxygen atoms to the metal center (vide ante). In the case of AfsNIR, the distances between Cu and nitrite oxygens are 2.2 and 2.3 Å [8]. In general two types of binding between nitrite ion and the Cu(II) or Cu(I) complex are known as nitrito- and nitro-modes (O-NO_2^- and N-NO_2^-, respectively) [73,74]. It has recently reported that the latter mode is thermodynamically favored in the Cu(I) complexes and the demonstration of quantitative NO evolution upon addition of two equivalents of protons to the Cu(I)(N-NO_2^-) complex suggests the substrate adduct having N-NO_2^- coordination as the most important enzyme intermediate [74]. However, all of the binding mode in NIR's interestingly are O-NO_2^- coordination. X-ray crystal analyses of NIR's suggested that two amino acid residues (Asp98 and His255) near the type 2 Cu site play an important role for nitrite reduction. On the basis of the structures of oxidized, reduced, nitrite-soaked oxidized, and nitrite-soaked AfsNIRs, Adman et al. have hypothesized, (1) that nitrite displaces a solvent bound to the type 2 Cu ion and forms a hydrogen bond to Asp98 with one of the two oxygen atoms; (2) that the proton in this hydrogen bond remains with Asp98 until the nitrite is reduced by one electron transferred from the type 1 Cu atom to the type 2 Cu atom; (3) that the N–O bond at the oxygen atom, hydrogen bonded to Asp98, breaks; and (4) that NO is released and the active site is restored [8]. The role of His255 might be to provide a hydrogen bond to water, which also hydrogen bonds to Asp98, in order to allow Asp98 to temporarily hold a hydrogen on the other carboxylate oxygen, during the displacement reaction of the solvent ligand with nitrite [7]. The RhsNIR mutant replaced the corresponding His with Glu showed a 100-fold loss of enzyme activity, and EPR and ENDOR measurements of the type 2 Cu center in the mutant demonstrated that nitrite does not bind to the copper site [42,75].

5. Conclusion

Copper NIR is a homotrimer, in which a monomer (ca. 36 kDa) contains one type 1 Cu (having 2His, Cys and Met ligands) and one type 2 Cu (having 3His and solvent ligands). The structures of the blue and the green type 1 Cu sites having electron-accepting function is distorted tetrahedral and flattened tetrahedral, respectively, and that of the type 2 Cu site catalyzing nitrite reduction is tetrahedral. The interatomic distance between the type 1 and 2 Cu's is 12.6 Å and these two Cu's are bound by the Cys-His sequence segment. The intramolecular electron transfer rate constant is ca. 2×10^3 s^{-1} at pH 6 and 25°C. The Cu NIR's interestingly bear some resemblance to cytochrome c,d_1-NIR's. The heme NIR's also contain two kinds of metal centers: c heme accepting an electron and d_1 heme relating to the catalytic reduction of nitrite. The shortest edge-to-edge distance between the c and d_1 hemes is 11 Å in a monomer [4]. The first-order rate constant of the intramolecular electron transfer process from the c heme site to the d_1 heme site in *Thiosphaera pantotropha* NIR is 1.4×10^3 s^{-1} at pH 7.0 [76].

Acknowledgements

This work was supported by Grant-in-Aid for Scientific Research on Priority Area (No. 10129217) from the Ministry of Education, Science, Sports and Culture. The authors appreciate the advice and help of Dr Kazuo Kobayashi and Professor Seiichi Tagawa, the Institute of Scientific and Industrial Research, Osaka University, in the pulse radiolysis of NIR's. The authors are grateful to Manabu Gohou, Masaharu Gotowda, and Hirotaka Watanabe for their help in X-ray crystal structure analysis, and thank Deligeer and Hiroshi Furusawa (Graduate School of Science, Osaka University) for assistance in preparing AxgNIR and determining the sequence alignment of it. They also acknowledge Professors Sohsuke Shidara (Faculty of Integrated Arts and Sciences, Hiroshima University), Hidekazu Iwasaki (Nagoya University of Foreign Studies), and Eiko Yabuuchi for useful discussions.

References

[1] W.G. Zumft, Microbiol. Mol. Biol. Rev. 61 (1997) 533.
[2] B.A. Averill, Chem. Rev. 96 (1996) 2951.
[3] R. Hille, Chem. Rev. 96 (1996) 2757.
[4] V. Fulop, J.W.B. Moir, S.J. Ferguson, J. Hajdu, Cell 81 (1995) 369.
[5] D. Nurizzo, M.C. Silvestrini, M. Mathieu, F. Cutruzzola, D. Bourgeois, V. Fulop, J. Hajdu, M. Brunori, M. Tegoni, C. Cambillau, Structure 9 (1997) 1157.
[6] J.W. Godden, S. Turley, D.C. Teller, E.T. Adman, M.Y. Liu, W.J. Payne, J. LeGall, Science 253 (1991) 438.
[7] E.T. Adman, J.W. Godden, S. Turley, J. Biol. Chem. 270 (1995) 27458.
[8] M.E.P. Murphy, S. Turley, E.T. Adman, J. Biol. Chem. 272 (1997) 28455.
[9] F.E. Dodd, S.S. Hasnain, Z.H.L. Abraham, R.R. Eady, B.E. Smith, Acta Crystallogr. D53 (1997) 406.

[10] (a) F.E. Dodd, J.Van Beeumen, R.R. Eady, S.S. Hasnain, J. Mol. Biol. 282 (1998) 369. (b) E. Suzuki, N. Horikoshi, T.Kohzuma, Biochem. Biophys. Res. Commun. 255 (1999) 427.
[11] N. Sakurai, T. Sakurai, Biochemistry 36 (1997) 13809.
[12] F. Neese, R. Kappl, J. Huttermann, W.G. Zumft, P.M.H. Kroneck, J. Biol. Inorg. Chem. 3 (1998) 53.
[13] T. Tsukihara, H. Aoyama, E. Yamashita, T. Tomizuka, H. Yamaguchi, K. Shinzawa-Itoh, R. Nakashima, R. Yano, S. Yoshikawa, Science 269 (1995) 1069.
[14] S. Iwata, C. Ostermeier, B. Ludwig, H. Michel, Nature 376 (1995) 660.
[15] M. Saraste, J. Castresana, FEBS Lett. 341 (1994) 1.
[16] J. van der Oost, A.P.N. de Boer, J.-W.L. de Gier, W.G. Zumft, A.H. Stouthamer, R.J.M. van Spanning, FEMS Microbiol. Lett. 121 (1994) 1.
[17] H. Iwasaki, T. Mori, J. Biochem. 42 (1955) 375.
[18] H. Iwasaki, S. Shidara, H. Suzuki, T. Mori, J. Biochem. 53 (1963) 299.
[19] (a) H. Iwasaki, T. Matsubara, J. Biochem. 71 (1972) 645. (b) H. Iwasaki, S. Noji, S. Shidara, J. Biochem. 78 (1975) 355.
[20] T. Kakutani, H. Watanabe, K. Arima, T. Beppu, J. Biochem. 89 (1981) 453.
[21] G. Denariaz, W.J. Payne, J. LeGall, Biochim. Biophys. Acta 1056 (1991) 225.
[22] K. Inatomi, L.I. Hochstein, Curr. Microbiol. 32 (1996) 72.
[23] D.J. Miller, P.M. Wood, J. Gen. Microbiol. 129 (1983) 1645.
[24] W.G. Zumft, D.J. Gotzmann, P.M.H. Kroneck, Eur. J. Biochem. 168 (1987) 301.
[25] E. Sawada, T. Satoh, H. Kitamura, Plant Cell Physiol. 19 (1978) 1339.
[26] S. Suzuki, T. Kohzuma, S. Shidara, K. Ohki, T. Aida, Inorg. Chim. Acta 208 (1993) 107.
[27] M. Masuko, H. Iwasaki, T. Sakurai, S. Suzuki, A. Nakahara, J. Biochem. 96 (1984) 447.
[28] M.-T. Liu, M.-C. Liu, W.J. Payne, J. LeGall, J. Bacteriol. 166 (1986) 604.
[29] T. Kakutani, H. Watanabe, K. Arima, T. Beppu, J. Biochem. 89 (1981) 453.
[30] E. Libby, B.A. Averill, Biochem. Biophys. Res. Commun. 187 (1992) 1529.
[31] Z.H.L. Abraham, D.J. Lowe, B.E. Smith, Biochem. J. 295 (1993) 587.
[32] E. Yabuuchi, I. Yano, S. Goto, E. Tanimura, T. Ito, A. Ohyama, Int. J. Syst. Bacteriol. 24 (1974) 470.
[33] T. Inoue, M. Gotoda, Deligeer, K. Kataoka, S. Suzuki, K. Yamaguchi, H. Watanabe, M. Goho, Y. Kai, J. Biochem. 124 (1998) 876.
[34] K. Yamaguchi, Deligeer, N. Nakamura, S. Shidara, H. Iwasaki, S. Suzuki, Chem. Lett. (1995) 353.
[35] K. Kataoka, M. Nakai, K. Yamaguchi, S. Suzuki, submitted.
[36] F.E. Dodd, S.S. Hasnain, W.N. Hunter, Z.H.L. Abraham, M. Debenham, H. Kanzler, M. Eldrige, R.R. Eady, R.P. Ambler, B.E. Smith, Biochemistry 34 (1995) 10180.
[37] J.A. Fee, Struct. Bonding 23 (1975) 1.
[38] S. Suzuki, Deligeer, K. Yamauchi, K. Kataoka, K. Kobayashi, S. Tagawa, T. Kohzuma, S. Shidara, H. Iwasaki, J. Biolog. Inorg. Chem. 2 (1997) 265.
[39] L. Ryden, in: R. Lontie (Ed.), Copper Protein and Copper Enzymes, vol. 1, CRC Press, Florida, 1984, p. 157.
[40] M. Kobayashi, H. Shoun, J. Biol. Chem. 270 (1995) 4146.
[41] W.P. Michalski, D.J.D. Nicholas, Biochim. Biophys. Acta 828 (1985) 130.
[42] K. Olesen, A. Veselov, Y. Zhao, Y. Wang, B. Danner, C.P. Scholes, J.P. Shapleigh, Biochemistry 37 (1998) 6086.
[43] A.A. DiSpirito, L.R. Taaffe, J.D. Lipscomb, A.B. Hooper, Biochim. Biophys. Acta 827 (1985) 320.
[44] G. Denariaz, W.J. Payne, J. LeGall, Biochim. Biophys. Acta 1056 (1991) 225.
[45] T. Sakurai, S. Suzuki, A. Nakahara, M. Masuko, H. Iwasaki, Chem. Lett. (1985) 1297.
[46] L.B. LaCroix, S.E. Shadle, Y. Wang, B.A. Averill, B. Hedman, K.O. Hodgson, E.I. Solomon, J. Am. Chem. Soc. 118 (1996) 7755.
[47] M. Kukimoto, M. Nishiyama, M.E.P. Murphy, S. Turley, E.T. Adman, S. Horinouchi, T. Beppu, Biochemistry 33 (1994) 5246.
[48] K. Kataoka, H. Furusawa, K. Yamaguchi, S. Suzuki, submitted.
[49] A.B. Glockner, A. Jungst, W.G. Zumft, Arch. Microbiol. 160 (1993) 18.

[50] R.W. Ye, M.R. Fries, S.G. Bezborodnikov, B.A. Averill, J.M. Tiedje, Appl. Environ. Microbiol. 59 (1993) 250.
[51] M. Nishiyama, J. Suzuki, M. Kukimoto, T. Ohnuki, S. Horinouchi, T. Beppu, J. Gen. Microbiol. 139 (1993) 725.
[52] F.F. Fenderson, S. Kumar, E.T. Adman, M.-Y. Liu, W.J. Payne, J. LeGall, Biochemistry 30 (1992) 7180.
[53] A. Toffanin, Q. Wu, M. Maskus, S. Casella, H.D. Abruna, J.P. Shapleigh, Appl. Environ. Microbiol. 62 (1996) 4019.
[54] I.E. Tosques, A.V. Kwiatkowski, J. Shi, J.P. Shapleigh, J. Bacteriol. 179 (1997) 1090.
[55] I.H.M. Vandenberghe, T.E. Meyer, M.A. Cusanovich, J.J. Van Beeumen, Biochem. Biophys. Res. Commun. 247 (1998) 734.
[56] J.M. Guss, H.D. Bartunik, H.C. Freeman, Acta Crystallogr. B48 (1992) 790.
[57] R.W. Strange, F.E. Dodd, Z.H.L. Abraham, J.G. Grossmann, T. Bruser, R.R. Eady, B.E. Smith, S.S. Hasnain, Nature, Struct. Biol. 2 (1995) 287.
[58] S. Suzuki, Deligeer, K. Yamaguchi, K. Kataoka, S. Shidara, H. Iwasaki, T. Sakurai, Inorg. Chim. Acta 276 (1998) 289.
[59] V. Ducros, A.M. Brzozowski, K.S. Wilson, S.H. Brown, P. Ostergaard, P. Schneider, D.S. Yaver, A.H. Pedersen, G.J. Davies, Nat. Struct. Biol. 5 (1998) 310.
[60] A. Messerschmidt, R. Ladenstein, R. Huber, M. Bolognesi, L. Avigliano, R. Petruzzelli, R. Rossi, A. Finazzi-Agro, J. Mol. Biol. 224 (1992) 179.
[61] I. Zaitseva, V. Zaitsev, G. Card, K. Moshkov, B. Bax, A. Ralph, P. Lindley, J. Biol. Inorg. Chem. 1 (1996) 15.
[62] H. Iwasaki, T. Matsubara, J. Biochem. 73 (1973) 659.
[63] M. Kukimoto, M. Nishiyama, T. Ohnuki, S. Turley, E.T. Adman, S. Horinouchi, T. Beppu, Protein Eng. 8 (1995) 153.
[64] T. Kohzuma, C. Dennison, W. McFarlane, S. Nakashima, T. Kitagawa, T. Inoue, Y. Kai, N. Nishio, S. Shidara, S. Suzuki, A.G. Sykes, J. Biol. Chem. 270 (1995) 25733.
[65] T. Kohzuma, S. Takase, S. Shidara, S. Suzuki, Chem. Lett. (1993) 149.
[66] M. Kukimoto, M. Nishiyama, M. Tanokura, E.T. Adman, S. Horinouchi, J. Biol. Chem. 271 (1996) 13680.
[67] S. Suzuki, T. Kohzuma, Deligeer, K. Yamaguchi, N. Nakamura, S. Shidara, K. Kobayashi, S. Tagawa, J. Am. Chem. Soc. 116 (1994) 11145.
[68] K. Kobayashi, Deligeer, S. Tagawa, S. Suzuki, J. Biochem. 126 (1999) 408.
[69] P. Kyritsis, A. Messerschmidt, R. Huber, G.A. Salmon, A.G. Sykes, J. Chem. Soc. Dalton Trans. (1993) 731.
[70] O. Farver, I. Pecht, Biophys. Chem. 50 (1994) 203.
[71] Z.H.L. Abraham, B.E. Smith, B.D. Howes, D.J. Lowe, R.R. Eady, Biochem. J. 324 (1997) 511.
[72] T. Kohzuma, S. Shidara, S. Suzuki, Bull. Chem. Soc. Jpn. 67 (1994) 138.
[73] N. Komeda, H. Nagao, Y. Kushi, G. Adachi, M. Suzuki, A. Uehara, K. Tanaka, Bull. Chem. Soc. Jpn. 68 (1995) 581.
[74] J.A. Halfen, S. Mahapatra, E.C. Wilkinson, A.J. Gengenbach, V.G. Young Jr., L. Que Jr., W.B. Tolman, J. Am. Chem. Soc. 118 (1996) 763.
[75] A. Veselov, K. Olesen, A. Sienkiewicz, J.P. Shapleigh, C.P. Scholes, Biochemistry 37 (1998) 6095.
[76] K. Kobayashi, A. Koppenhofer, S.J. Ferguson, S. Tagawa, Biochemistry 36 (1997) 13611.